Astrophysical S factor for the ^{11}B$(d, n)^{12}$C reaction below 135 keV

Y. Parpottas,[1,2] M. W. Ahmed,[1,2] M. A. Blackston,[1,2] R. H. France III,[1,3] B. A. Perdue,[1,2] R. M. Prior,[1,4] A. Sabourov,[1,2] M. C. Spraker,[1,4] and H. R. Weller[1,2]

[1]*Triangle Universities Nuclear Laboratory, Durham, North Carolina 27708, USA*

[2]*Department of Physics, Duke University, Durham, North Carolina 27708, USA*

[3]*Department of Chemistry and Physics, CBX 82 Georgia College and State University Milledgeville, Georgia 31061, USA*

[4]*Department of Physics, North Georgia College and State University, Dahlonega, Georgia 30597, USA*

(Received 19 April 2006; published 19 July 2006; corrected 28 July 2006)

The ^{11}B$(d, n)^{12}$C reaction was studied using deuteron beams of 120–160 keV to determine the absolute astrophysical S factors and cross sections for the n_0 and n_1 neutron groups. The slopes of the S factors are consistent with zero for both the n_0 and n_1 cases. The measured S factor for the sum of both neutron groups at c.m. energies below 135 keV is $S = 3180 \pm 480$ keV b. A DWBA calculation is able to reproduce the ratio of the S factors found here to those obtained in a recent study of the ^{7}Li$(d, n_{0,1})^{8}$Be reaction.

DOI: 10.1103/PhysRevC.74.015804 PACS number(s): 21.10.Jx, 24.10.Ht, 25.45.Hi

I. INTRODUCTION

The primordial abundances of the light nuclei have been considered to be the important observable that probes the physical environment of the early Universe in the framework of big-bang cosmology. One of the successes of the standard big-bang nucleosynthesis model is the determination of the baryon number density that occurs during the process of nucleosynthesis. The production of elemental carbon-nitrogen-oxygen (CNO) in inhomogeneous scenarios of big bang nucleosynthesis is very important for cosmological model calculations. The main channel to CNO elemental production in models with $\Omega_b = 1$ (the ratio of the baryonic density to the critical energy density) is the ^{7}Li$(n, \gamma)^{8}$Li$(\alpha, n)^{11}$B$(n, \gamma)^{12}$B$(\beta^{-}\nu)^{12}$C reaction sequence [1]. The authors of Ref. [1] point out that the ^{7}Li$(\alpha, \gamma)^{11}$B reaction is competitive at lower values of Ω_b. In this sequence neutron capture on ^{11}B followed by β decay of ^{12}B leads to ^{12}C. Because estimates [1] indicate that the ^{11}B$(d, n)^{12}$C reaction may very well be competitive, measurements of this reaction down to astrophysical energies are of interest.

Cross sections and angular distributions for the n_0 and n_1 neutron groups of the ^{11}B$(d, n)^{12}$C reaction have been reported for center-of-mass (c.m.) energies down to 370 keV [2]. The data were taken using a single stilbene crystal counter and are consistent with direct-reaction theory [3]. They also agree, within experimental error, with the relative intensities of the n_0 and n_1 groups of Ref. [4]. The present measurements were undertaken at lower c.m. energies (94–127) keV. The absolute cross section and the slope and magnitude of the S factor were determined for the n_0 transition to the ground state of ^{12}C (0^{+}) and for the n_1 transition to the (2^{+}) first excited state.

II. EXPERIMENTAL DETAILS

The ^{11}B$(d, n)^{12}$C reaction was studied using the Triangle Universities Nuclear Laboratory's (TUNL) 80-keV atomic beam polarized ion source (ABPIS). The target chamber could be biased up to -80 keV to increase the beam energy to 120, 140, and 160 keV. Although the measurements were performed using a vector polarized beam, the present results are concerned only with the unpolarized yields that were obtained by combining the "spin-1" and the "spin-2" yields. Analyzing powers were also obtained and will be the subject of a future publication. The transitions used for these measurements generated a pure vector polarized beam (p_z only with $p_{zz} = 0$). The Wien filter [5] was used to set the spin symmetry axis along the x direction (i.e., perpendicular to the reaction plane) at the location of the target. The beam was switched between the two spin states at a rate of 10 Hz. The data were sorted into spin-1 and spin-2 spectra.

Beam currents averaged about 20 μA, and the data sets were taken in a 2-week long run. The current was measured and integrated using a setup that converted the current to a light signal that was propagated via a fiber-optic cable from the high-voltage target to ground potential. Its accuracy was determined to be better than $\pm 1\%$ by observing the result obtained using a precision calibrated current source instead of the beam.

The beam was stopped in the target. The 1-mg/cm^2 enriched (99.5%) ^{11}B targets were evaporated onto 3-mm-thick copper backings by ACF-Metals Co. [6]. Several targets were utilized to minimize any effects of target deterioration and/or surface contamination.

Neutrons were detected in six 12.7-cm-diameter and three 11.4-cm-diameter BC501A liquid scintillators of 5.1 cm thickness. The 12.7-cm-diameter detectors were placed approximately 40 cm from the target face with their centers at angles of 0°, 22.5°, 45°, 67.5°, 90°, and 90°. The 11.4-cm diameter detectors were placed approximately 60 cm from the target face with their centers at angles of 112.5°, 135°, and 150° on the opposite side of the target chamber. Pulse-shape discrimination (PSD) techniques were utilized to enable separation of neutrons from gammas. An accurate determination of the detector efficiencies was achieved using previous calculations [7] and measurements [8,9]. These efficiency calculations were well modeled for given fractions of the ^{137}Cs edge using the Physikalisch-Technische Bundesanstalt (PTB) group's Monte Carlo programs NRESP7 and NEFF7;

in our case the thresholds were set at 1.0 times the ^{137}Cs edge (defined to be the point at which the yield falls to one-half its peak value). The overall uncertainty in the detector efficiencies used here is estimated to be $\pm 3\%$.

Response functions for each type of detector and for each detected neutron group energy are necessary to fit the spectra and extract the yields. These functions were previously measured in TUNL's Shielded Source Area (SSA) using monoenergetic neutron beams produced via the ^{2}H$(d, n)^3$He reaction. Time-of-flight techniques were used to separate the monoenergetic ^{2}H$(d, n)^3$He neutrons from the lower-energy continuum neutrons generated by breakup reactions. In addition to the neutron groups from the ^{11}B$(d, n)^{12}$C reaction, a neutron group from the ^{2}H$(d, n)^3$He reaction was also evident in the spectra. This background peak was identified by studying the rise in its yield in conjunction with the integrated beam current, corresponding to the buildup of deuterium in the target. The response function for neutrons from the ^{2}H$(d, n)^3$He reaction at $E_d = 80$ keV was measured by implanting deuterium into a blank titanium target [10].

III. DATA ANALYSIS

A. Yields

The neutron spectra with PSD cuts for each angle and each deuteron spin-state were fitted with a combination of the measured n_0, n_1, n_2 and ^{2}H$(d, n)^3$He response functions as shown in Fig. 1. The n_0 yields were obtained by subtracting the n_1, n_2 and the ^{2}H$(d, n)^3$He functions from the spectrum and then summing the remaining spectrum from approximately 3 MeV up to the end point of the n_0 group. A correction factor was also obtained to account for the fact that the yields were not summed over the entire response function. This factor, a multiplicative factor used to correct the efficiency, was equal to the sum of the response function over the region summed for the data divided by the sum of the entire response function. A similar procedure was performed to obtain the n_1 and n_2 yields. Typical values for the above correction factor in the case of the n_0 and n_1 groups were of the order of 60%–70%; values for the n_2 group were of the order of 10%–15%. Extraction of the n_2 yields could be unreliable because of the small percentage of the usable n_2 spectrum. Therefore, only the n_0 and n_1 groups were considered for further analysis. The above fitting procedure was also repeated with a combination of the n_0 and n_1 response functions from approximately 6 MeV up to the end point of each neutron group. In this case, the correction factor for the n_0 and n_1 groups was 40%–50%. The resulting yields agreed with the yields computed by fitting all neutron peaks.

Polarized yields for each angle and each neutron group were summed to obtain the unpolarized yields. For a vector-polarized beam, the yield observed is defined as follows [11]

$$Y_i(\theta, E) = Y(\theta, E)\left[1 + \frac{3}{2} p_{zi} A_y(\theta, E)\right], \tag{1}$$

where Y_i is the polarized yield for spin state i (1 or 2), Y is the unpolarized yield, p_{zi} is the vector polarization value for each spin state, and A_y is the vector analyzing power. The unpolarized yield is then written as

$$Y(\theta, E) = \frac{p_{z2} Y_1(\theta, E) - p_{z1} Y_2(\theta, E)}{p_{z2} - p_{z1}}. \tag{2}$$

The angle-dependent yields for each neutron group were normalized by the detector efficiency, the correction factor

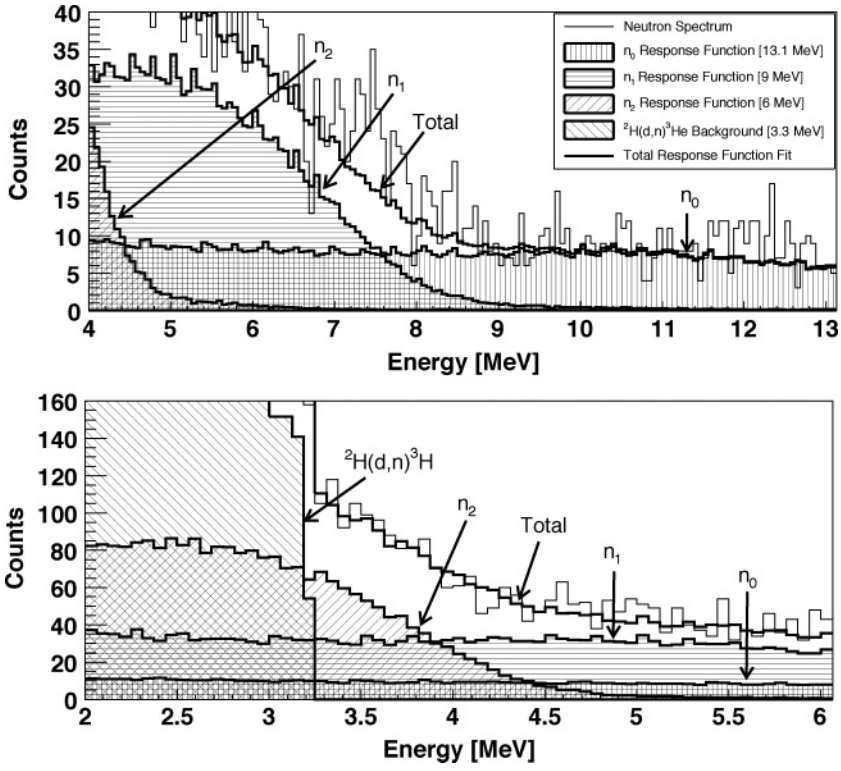

FIG. 1. The measured neutron spectrum for the ^{11}B$(d, n)^{12}$C reaction at an incident energy of 120 keV in the fitting region between 3–13.5 MeV; the top panel shows the high-energy end of the fitting region and the bottom panel shows the low-energy end. The energy calibration used for the x axis was determined by using the end-point channel of the n_0 state at 13.2 MeV and is uncertain to ± 0.5 MeV.

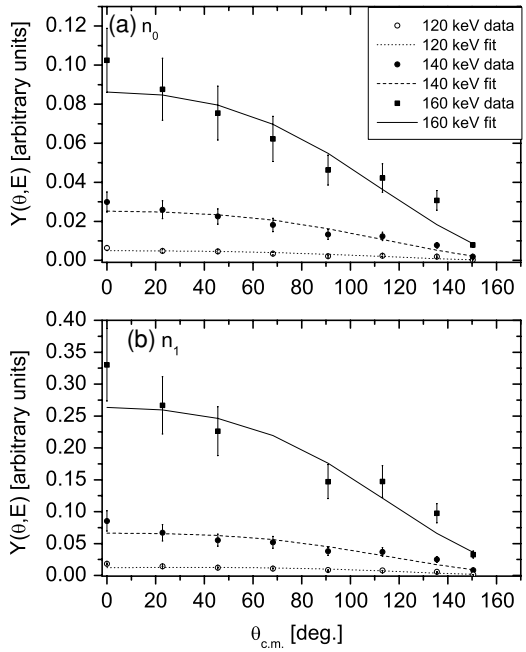

FIG. 2. The angle-dependent yields for each energy and each neutron group and the corresponding Legendre polynomial fits. The error bars represent the statistical and systematic errors associated with the data points.

described above, the fraction of the solid angle subtended by the detector, and the total number of incident deuterons. The angular distribution for each neutron group was then fitted to an expansion in terms of Legendre polynomials to obtain the angle-integrated yields at each energy. The data and the polynomial fits (to order $k = 2$) are shown in Fig. 2.

B. *S* factor

The measured energy-dependent yield because of the beam stopping in the target is the total yield from the beam energy (E_d) to zero and can be written as

$$Y(E_d) = C \int_{E_d}^{0} \frac{\sigma(E)}{\mathrm{STP}(E)}\, dE, \tag{3}$$

where $\sigma(E)$ is the energy-dependent cross section and STP(E) is the stopping power of the target for deuterons. The constant C is the product of the total number of incident deuterons, the detector efficiency, the correction factor discussed above and the fraction of the solid angle subtended by the detector. In Eq. (3), the cross section can be written in terms of the astrophysical $S(E)$ factor as

$$\sigma(E_{\mathrm{c.m.}}) = \frac{S(E_{\mathrm{c.m.}})}{E_{\mathrm{c.m.}}}\, e^{-2\pi\eta}, \tag{4}$$

where η is the Sommerfeld parameter and $2\pi\eta = 31.29 Z_1 Z_2 (\mu/E_{\mathrm{c.m.}})^{1/2}$. Z_1 and Z_2 are the projectile and target charges, respectively, μ is the reduced mass in amu, and $E_{\mathrm{c.m.}}$ is the center-of-mass energy in keV. At these low energies, the S factor was assumed to be a linear function of energy:

$$S(E_{\mathrm{c.m.}}) = S_0 + S_1 E_{\mathrm{c.m.}}. \tag{5}$$

TABLE I. Comparison of the yield ratios for a theoretical calculation assuming $S(E)$ is constant and the experimental ratios for the n_0 and n_1 neutron yields.

Yield ratio[a]	Theoretical	Experimental	
		n_0	n_1
$Y(160)/Y(140)$	3.56	3.4 ± 0.55	3.9 ± 0.56
$Y(140)/Y(120)$	4.76	5.2 ± 0.77	4.75 ± 0.6

[a] $Y(160)$, $Y(140)$, and $Y(120)$ are the yields at beam energies of 160, 140, and 120 keV, respectively.

The yields for a given beam energy can be calculated for any given values of S_0 and S_1 using Eq. (3). An evaluation of the yield ratios at different energies was performed using the integral in Eq. (3) and assuming a constant S factor. A comparison with the corresponding experimental yield ratios provided insight into the energy dependence of the S factor. Table I shows these theoretical and experimental yield ratios for each neutron group. The results indicate that the S factor for both the n_0 and the n_1 groups is consistent with the assumption of a constant value within the experimental uncertainties.

In addition, the measured yields at energies of 120, 140, and 160 keV were fitted simultaneously to determine the best fit parameters (S_0 and S_1) by evaluating the integrals in Eq. (3). For this purpose, the target was divided into 1-μg/cm^2 layers, each of which corresponded to an energy loss of less than 1 keV in the target material. The stopping power of the target was calculated using the energy loss equations of Anderson and Ziegler [12]. The yield for the first layer was then calculated using arbitrary starting values of S_0 and S_1. The energy loss for the layer was calculated, and the yield calculation was repeated for the next layer at the decreased energy. This process was repeated until the yield of a layer was less than 0.1% of the yield for the first layer. The total yield at that beam energy was the sum of the yields from all the layers of the target. This process was performed for all three beam energies and repeated iteratively, continuously adjusting the values of S_0 and S_1 until the best fit to the measured yields was obtained. The calculated yields and the constant C in Eq. (3) were used to determine the absolute S factor and, subsequently, the absolute cross section from Eq. (4). Errors in the values of S_0 and S_1 include both the statistical uncertainties associated with the experimental yields (10%) and the systematic ones from the response function fits to the spectra (15%), from the S factor fits to the three yields (5%), and from the parameters necessary to determine the absolute scale (4%).

IV. RESULTS AND DISCUSSION

Figure 3 shows the measured yields as a function of beam energy for the ground-state and the first-excited-state transitions. The error bars represent the statistical errors from the raw yields and the systematic errors generated from fitting the response functions to the spectra. The two curves in each plot are the calculated yields obtained after fitting the measured yields assuming the S factor is constant with energy

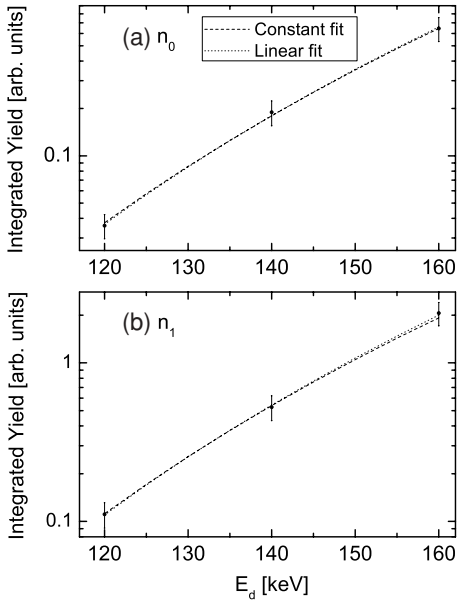

FIG. 3. Measured energy-integrated yields in arbitrary units for the ^{11}B$(d, n_0)^{12}$C and ^{11}B$(d, n_1)^{12}$C plotted at the incident beam energy. The error bars include statistical and systematic uncertainties. The curves were obtained from the fitting procedure described in the text assuming a constant or a linear S factor.

or varies linearly. The numerical values of the S factors and the corresponding χ^2 values of the fits are given in Table II. The results for both transitions (n_0 and n_1) are consistent with a zero slope. The values for a constant S factor are adopted for both the n_0 and n_1 transitions and, therefore, the S factor value for the n_0 plus the n_1 transitions is 3180($\pm$480) keV b.

Cross sections were calculated from the constant S factor values obtained from the numerical integration of Eq. (3) for each effective center-of-mass energy and each neutron group. The effective energy is defined as the energy of the beam in the target that has given rise to one half of the total yield. The results are shown in Table III. The total cross sections ($\sigma_{n_0+n_1}$) along with a curve resulting from Eq. (4) with $S = 3180$ keV b are shown in Fig. 4.

To lend credibility to the present results, a comparison of the S factor values from the present measurements with those obtained in a recent similar study of the ^{7}Li$(d, n)^8$Be reaction [10] was performed. The cross section of the n_0 group from each reaction was calculated at $E_{\text{c.m.,eff.}} = 110$ keV using the DWBA formalism and the code DWUCK4 [13]. Note that the ground and the first excited states of the ^{7}Li and the ^{8}Be nuclei have J^π values that are identical to

TABLE II. Numerical values for the constant and linear $S(E)$ fits to the experimental yields.

Neutron group	$S(E) = S_0 + S_1 E$ [keV b]	χ^2
n_0	$S(E) = 800(\pm 150)$	0.09
	$S(E) = 670(\pm 180) + 1.1(\pm 1.3)E$	0.15
n_1	$S(E) = 2380(\pm 460)$	0.1
	$S(E) = 1900(\pm 990) + 4.6(\pm 14.0)E$	0.12

TABLE III. Numerical values for the absolute cross section of n_0 and n_1 neutron groups as computed from $S(E) = S_0$ values.

$E_{\text{c.m.,eff.}}$ [keV]	$\sigma_{\text{Total}}(E_{\text{c.m.,eff.}})[\mu\text{b}]$	
	n_0	n_1
94	0.0066 ± 0.0011	0.0193 ± 0.0036
110	0.0279 ± 0.0058	0.0812 ± 0.0164
127	0.0903 ± 0.0167	0.2697 ± 0.0540

those of the ^{11}B and ^{12}C nuclei. Furthermore, viewed as a stripping reaction, the transferred proton is a $1p_{3/2}$ proton for the n_0 channel in both reactions and a $1p_{1/2}/1p_{3/2}$ proton for the n_1 case. The potentials of Ref. [14] were used for the cross-section calculation in the case of the ^{7}Li$(d, n)^8$Be reaction and the potentials of Refs. [15–17] were used for the ^{11}B$(d, n)^{12}$C reaction. The single-particle wavefunctions were found by adjusting the well depth of a Wood-Saxon potential to reproduce the appropriate experimental binding energies. The DWUCK4 cross section (σ_{DWBA}) is related to the actual cross section as follows

$$\sigma(E_{\text{c.m.}}) = \frac{2J_R + 1}{2J_T + 1} \frac{S_{lj}}{2j + 1} \frac{D_0^2}{10^4} \sigma^{lsj}_{\text{DWBA}}(E_{\text{c.m.}}), \qquad (6)$$

where J_R is the total angular momentum of the residual nucleus, J_T is the total angular momentum of the target nucleus, j is the total angular momentum of the transferred single particle, S_{lj} is the spectroscopic factor for a specific l and j, and D_0^2 is the zero-range approximation of the overlap function. For deuterons, $D_0^2 \approx 1.5 \times 10^4$ MeV fm^3 [13]. An experimental value for the spectroscopic factor of the n_0 group was adopted from Ref. [18] and theoretical values were adopted for the other spectroscopic factors from Ref. [19]. Using Eqs. (4) and (6), we then calculated the S factor ratio of the ^{7}Li$(d, n_0)^8$Be reaction to the ^{11}B$(d, n_0)^{12}C$ reaction to be 0.55. The corresponding experimental ratio of these two S factors is 0.53 ± 0.18. Similarly, the theoretical ratio for the n_1 group is 1.1 and the experimental ratio is 1.3 ± 0.4. We see that the predicted ratios of the S factors for the ^{7}Li$(d, n)^8$Be reaction to the S factors for the ^{11}B$(d, n)^{12}$C reaction are in agreement with the experimental results.

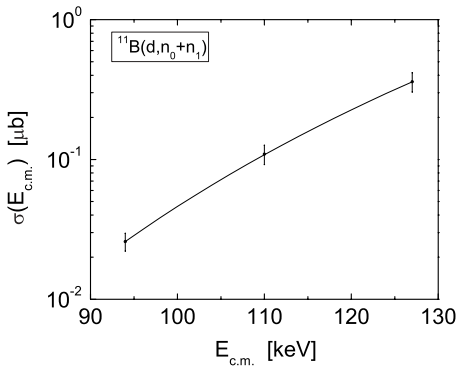

FIG. 4. The total cross sections and the resulting curve from Eq. (4) with $S = 3180$ keV b. The error bars indicate the statistical and systematic uncertainties associated with the data points.

V. CONCLUSION

The neutrons leading to the ground state and the first excited state in the $^{11}B(d,n)^{12}C$ reaction were measured to obtain the S factors and the cross sections for these reactions at c.m. energies below 135 keV. The measured S factor for the sum of the n_0 and the n_1 neutron groups in the $^{11}B(d,n)^{12}C$ reaction was found to be constant and equal to 3180 ± 480 keV b at these energies.

A comparison of the S factor ratio of the $^{7}Li(d,n_{0,1})^{8}Be$ reaction to the $^{11}B(d,n_{0,1})^{12}C$ reaction obtained using the DWBA formalism to the ratios obtained using the experimental results of the present work along with those of Ref. [10] shows reasonably good agreement, thus lending confidence to the present results.

ACKNOWLEDGMENTS

This work was partially supported by the U.S. D.O.E under grants DE-FG02-97ER41046, DE-FG02-97ER41033, and DE-FG02-97ER41042.

[1] L. H. Kawano, W. A. Fowler, R. W. Kavanagh, and R. A. Malaney, Astrophys. J. **372**, 1 (1991).
[2] O. Ames and G. E. Owen, Phys. Rev. **109**, 1639 (1958).
[3] G. E. Owen and L. Madansky, Phys. Rev. **105**, 1766 (1957).
[4] A. Ward and P. J. Grant, Proc. Phys. Soc. A **68**, 637 (1955).
[5] A. J. Mendez, C. D. Roper, J. D. Dunham, and T. B. Clegg, Rev. Sci. Instrum. **67**, 3073 (1996).
[6] ACF-Metals, Tuscon, AZ, USA.
[7] G. Dietz and H. Klein, *NRESP4 and NEFF4 Monte Carlo Codes for the Calculation of Neutron Response Functions and Detection Efficiencies for NE213 Scintillation Detectors* (Physikalisch-Technische Bundesanstalt, Bundesallee 100, W-3300 Braunschweig, 1982).
[8] D. E. Gonzalez Trotter, Ph.D. thesis, Duke University, 1997.
[9] F. Salinas Meneses, Ph.D. thesis, Duke University, 1998.
[10] A. Sabourov *et al.*, Phys. Rev. C **73**, 015801 (2006).
[11] H. H. Barschall, *Polarization Phenomena in Nuclear Reactions*, (University of Wisconsin Press, Madison, Winconsin, 1971), p. xxv.
[12] H. H. Anderson and J. F. Ziegler, *Hydrogen Stopping Powers and Ranges in All Elements* (Pergamon, London, 1977).
[13] P. D. Kunz, University of Colorado, Boulder, CO, *http://spot.colorado.edu/∼kunz/DWBA.html*
[14] R. B. Galloway and A. M. Ghazarian, Phys. Rev. C **29**, 2349 (1984).
[15] M. B. Chadwick and P. G. Young, Nucl. Sci. Eng. **123**, 17 (1996).
[16] O. Karban, J. Lowe, and P. D. Greaves, Nucl. Phys. **A133**, 255 (1969).
[17] W. Fitz, R. Jahr, and R. Santo, Nucl. Phys. **A101**, 449 (1967).
[18] G. H. Neuschaefer, M. N. Stephens, S. L. Tabor, and K. W. Kemper, Phys. Rev. C **28**, 1594 (1983).
[19] S. Cohen and D. Kurath, Nucl. Phys. **A101**, 1 (1967).